VELOCITY FIELD AROUND DARRIEUS WIND TURBINE ROTOR USING ACTUATOR CELL MODEL AND OTHER CFD METHODS

KRZYSZTOF ROGOWSKI AND KLAUDIA ROGOWSKA

Warsaw University of Technology
The Institute of Aeronautics and Applied Mechanics
Nowowiejska 24, 00–665 Warsaw, Poland

(received: 4 May 2018; revised: 11 June 2018;
accepted: 29 June 2018; published online: 6 July 2018)

Abstract: The main purpose of this work is to analyze the usefulness of the active cell model (ACM) developed by the author of this article to estimate the flow field around a single-bladed vertical-axis wind turbine (VAWT) with the Darrieus-type rotor. The obtained flow velocity fields were compared with the experimental values taken from the literature available on the Internet. Additionally, the flow fields around the rotor and the aerodynamic forces were determined using the following approaches: the k-ε RNG turbulence model, the scale-adaptive simulation (SAS) and the laminar model. The velocity profiles behind the turbine rotor obtained with all numerical approaches are consistent with the experiment. The aerodynamic blade loads obtained using numerical methods also appear to be satisfactory.

Keywords: CFD, vertical-axis wind turbine, aerodynamic blade loads, wake modeling
DOI: https://doi.org/10.17466/tq2018/22.3/d

1. Introduction

1.1. Vertical-axis wind turbines

Even though the share of the vertical-axis wind turbine (VAWT) is currently decreasing in Poland, the number of patents related to them continues to increase. There is also a growing interest in this topic in the world as evidenced by the number of publications.

The archetype of the VAWT is considered to be a Persian windmill (Figure 1a) from the 2nd century BC used to drive a quern. This device resembled a water wheel in which half of the rotor was shielded from the wind. The source of torque in these devices was the drag difference on the windmill blades. Such turbines are called drag-driven devices [1].

Devices with the Darrieus rotor operate on a completely different principle. Darrieus wind turbines are an alternative to traditional horizontal-axis propeller-type machines. This lift-driven device proposed by a French aeronautical engineer, Georges Jean Marie Darrieus was patented by U. S. Patent Office in 1931 [2]. According to the inventor, the rotor should have properly curved blades. The shape of this curvature should be close to a rotating rope. This shape is called the Troposkien shape (from Greek: στροφή – turning; σχοινί – rope). A rotor blade having such a shape only transfers the tensile and compressive stresses. The aerodynamic torque in this device comes from an aerodynamic force generated on the rotor blades that have aerodynamic profiles. The silhouette of a typical two-bladed Darrieus wind turbine is shown in Figure 1b. There are also modifications of this rotor, Figure 1c shows, for example, a rotor with straight blades. It is a VAWT created in 1980 in the well-known company McDonnell Douglas. The French engineer's idea was forgotten for almost half a century, then it was discovered in the mid-1970s, mainly in the USA and Canada. At that time, extensive research work was undertaken, resulting in the creation of wind farms in California in Tehachapi, Altamont Pass and San Gorgonio. About 500 machines of this type were built there with the rated powers of 150–300 kW. In 1987, the largest wind turbine of this type was built – the Canadian EOL with an installed capacity of 3.8 MW [1].

The Darrieus concept was again forgotten when the idea of floating wind turbines appeared in recent years. The low centre of gravity of the rotor is the reason why the Darrieus wind turbine is better for offshore applications than a traditional wind turbine with a horizontal axis of rotation [3].

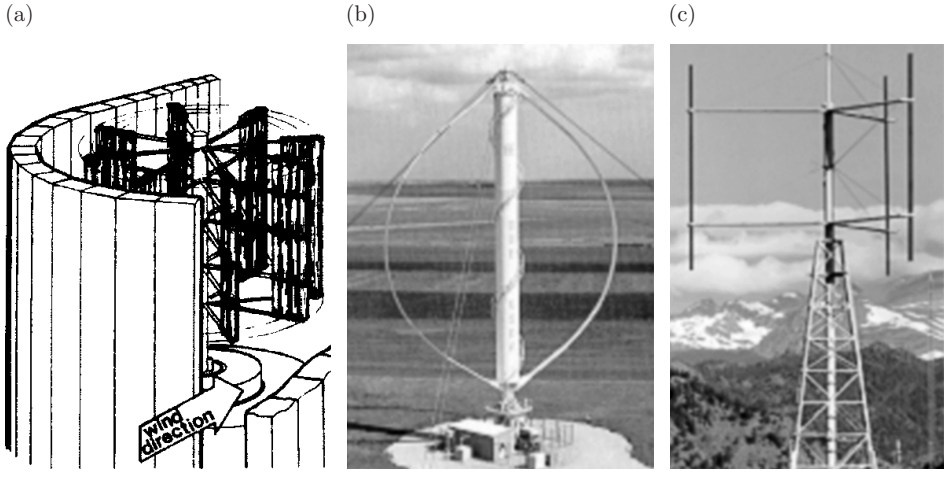

Figure 1. (a) Persian windmill silhouette [1]; (b) Darrieus wind turbine [1]; (c) H-type Darrieus wind turbine [1]

1.2. State of the art

Currently, the most well-known tool for analyzing the aerodynamic performance of the Darrieus rotor is the double-multiple streamtube (DMS) model. It is a method that uses two actuator disks working in tandem. One of these disks represents the upwind part of the rotor and the second the downwind part. This method takes into account one component of the flow only, therefore, it is suitable for rotors with low solidity. The calculation of aerodynamic forces is possible due to the combination of the actuator disc theory with the blade element theory [4]. However, the aerodynamic blade loads obtained with this method are not satisfactory [5]. Strickland *et al.* [6] proved in their report that an aerodynamic wake is determined wrongly when these methods are used. The same authors have developed a much more accurate approach based on vortex equations. This approach is still used, but it is more computationally expensive. An interesting approach is the actuator cylinder model developed by Madsen [3]. In this approach the curvilinear surface is used instead of a flat surface of the actuator disc as in the case of the DMS approach. On this circular surface Volume forces are applied in the radial direction.

Nowadays Computational Fluid Dynamics (CFD) methods have been developed very strongly. They solve the average Navier-Stokes equations whereas turbulence is solved by means of additional models called turbulence models. However, these methods are very costly computationally because they require modeling using dense grids [7, 8]. Although the rotor calculation shown in Figures 1b or 1c is theoretically possible using CFD methods, this is not usually done. This is because these methods incorrectly determine the critical attack angle [9]. In addition, the use of a large number of processors is not economical. This determines the need to look for new solutions. The presented article is an extended version of Rogowski's article [10]. The article presents a comparison of speed distributions obtained by means of various numerical approaches and the actuator cell model (ACM) approach developed by Rogowski [10].

2. Wind turbine

2.1. Wind turbine rotor

The wind turbine rotor presented in this paper consists of only one straight blade with the NACA 0012 airfoil. The chord length of the airfoil, c, is 9.14 cm. The rotor radius, R, was established to be 0.61 m giving the rotor solidity, $\sigma = c/R$, of 0.15. The most important parameter determining the rotor operation is the so called tip speed ratio, *TSR*. This parameter is defined as a non-dimensionless ratio of the rotor blade velocity (the tangential velocity of the blade), V_t, to the undisturbed flow velocity, V_0. The tip speed ratio can be written as:

$$TSR = \frac{V_t}{V_0} = \frac{\omega R}{V_0} \tag{1}$$

where: ω is the angular velocity of the rotor. In the case of the examining rotor the tip speed ratio value is 5.0. This means that the tangential velocity of the rotor is

five times larger than the undisturbed flow velocity. According to Paraschivoiu [4], the optimum value of the rotor power coefficient, c_p, for rotors that have a low solidity value ($\sigma \leq 0.15$) is obtained for *TSR*s of 4–5. The rotor power coefficient is defined as:

$$c_p = \frac{power\ extracted\ by\ rotor}{power\ available\ in\ flow\ stream} \tag{2}$$

For a typical Darrieus-type rotor, the maximum value of c_p is around 0.4. Therefore, in these simulations a rotor operating at the optimal *TSR* was tested. For optimal *TSR*s, the so called, secondary effects are negligible [4]. Moreover, local angles of attack do not exceed static critical angles of attack, thanks to this, the phenomenon of dynamic stall does not appear. According to Paraschivoiu [4] the secondary effects are associated with *e.g.*: the presence of struts, the rotor geometry, the presence of spoilers, *etc.* During simulations the angular velocity of the rotor was 0.75 rad/s and the undisturbed flow velocity was 0.091 m/s.

The numerical experiment performed in this work corresponds to the experiment of Strickland *et al.* [6]. This experiment was performed in a water towing tank. The selected operating fluid was water due to the lower angular velocity of the rotor at the same tip speed ratio. In addition, studies conducted in water made it easier to visualize the flow field. More information about the experiment settings can be found in two reports and in a scientific article [6, 11, 12]. Figure 2 presents a sketch of a one-bladed rotor.

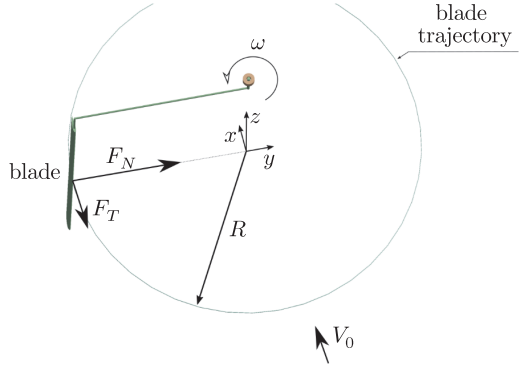

Figure 2. Silhouette of one-bladed vertical axis wind turbine

2.2. Aerodynamic characteristics of the rotor

The Darrieus wind turbine is a lift-driven device consisting of a number of curved blades. A rotor with straight blades can be called a Darrieus-type rotor. The principle of the rotor operation results from the creation of a lifting force on its blades. The local velocity at the rotor, V, is lower than the undisturbed flow velocity. The relative velocity, W, is the sum of the vector of the tangential velocity of the blade and the velocity vector V. The angle between the relative velocity vector and the chord line is called the angle of attack, α. This angle changes with the azimuth angle, θ, and depends on the tip speed ratio and the

blade Reynolds number. The azimuth angle θ uniquely determines the position of the rotor and is measured as shown in Figure 3. The direction of the drag is the same as the direction of the relative velocity W, whereas the lift force is perpendicular to this velocity. The aerodynamic force components, the lift force and the drag, projected onto the normal and tangent directions give the normal and tangential forces, respectively.

During the experiments of Strickland *et al.* [6] both aerodynamic blade loads as well as velocity profiles behind the rotor were measured. The velocity profiles were measured at the distance of one rotor diameter downstream behind the rotor, as shown in Figure 3. The wake velocity component V_x is normalized by the undisturbed flow velocity V_0.

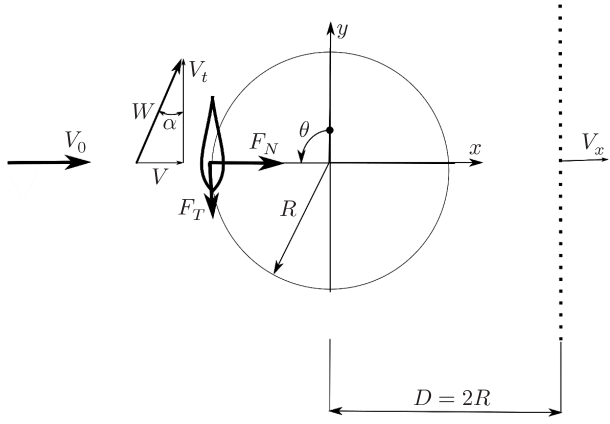

Figure 3. Two-dimensional rotor model; forces acting on the rotor blade and velocity vectors

3. Methods

In this work, numerical methods were used to assess the aerodynamic properties of the rotor: aerodynamic forces and flow parameters in the rotor area. The classic full CFD approaches were used as well as the method developed by Rogowski [10] – the Actuator Cell Model (ACM).

3.1. Full CFD approach

The full CFD approach, for the purposes of this article, means the numerical approach in which the boundary layer is modeled using a turbulence model and an appropriate grid near the blade edges. The flow around the Darrieus rotor (or a Darrieus-type rotor) cannot be considered as steady. Fluctuations in the rotational torque of a one-, two-and even three-bladed rotor are so large that the flow must be considered as unsteady. Therefore, the moving mesh technique was utilized in all simulations. In this concept, the rotor is surrounded by a large square stationary area, a computational domain. Moreover, there is a smaller circular area in the vicinity of the turbine rotor which rotates during the simulation with the same angular velocity as the rotor. The data between these two areas is

exchanged via the interface. Rogowski *et al.* proved in their previous works [13, 14] that the ratio of the square side length to the rotor diameter should be at least 10. Otherwise, the power coefficient results may be somewhat overstated. Interestingly, the result obtained by Rogowski *et al.* [13, 14] is right both for drag-driven rotors (such as *e.g.* Savonius rotors) as well as for Darrieus-type rotors. Figure 4 shows schematically the concept of the numerical approach and the boundary conditions: the velocity inlet, the pressure outlet, the walls, and the symmetry. The symmetry boundary condition can be used as a zero-shear stress wall boundary condition.

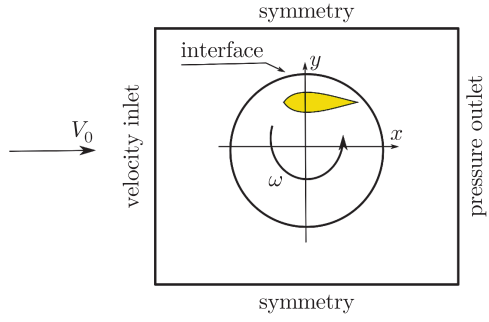

Figure 4. Numerical approach and boundary conditions

In all the cases presented in this article, the rotor was modeled as a two-dimensional object consisting of one airfoil rotating with respect to the axis of rotation. In the two examined cases, the two-dimensional Navier-Stokes (NS) equations were taken into account for the RNG k-ε turbulence model and for the laminar model. In the case of the Scale-Adaptive Simulation approach, the two-dimensional flow was considered using three-dimensional NS equations. Therefore, the presented approach is essentially a 2.5D approach.

As mentioned in the previous paragraph, one of the approaches used was the k-ε RNG turbulence model. This model solves two variables: the turbulence kinetic energy and the rate of its dissipation. This approach was developed using the so called Re-Normalization Group methods, hence, the acronym RNG.

In the laminar approach, no turbulence model is considered. Two equations of momentum and equation of continuity are solved only. Therefore, the presented approach can be treated as a direct numerical simulation (DNS) approach.

The scale-adaptive simulation (SAS) model is an improved unsteady-averaged Navier-Stokes (URANS) approach. It enables the solution of a turbulent spectrum in an unstable flow. This is a model developed on the well-known shear stress transport (SST) formulation.

More about the models used can be found, for example, in the ANSYS Fluent documentation.

3.2. Actuator cell concept

The actuator cell model (ACM) is an original approach developed by Rogowski [10]. Thanks to the moving mesh technique, it is also a model that allows analyzing unsteady flows. In this approach, the boundary layer around the airfoil of the rotor blade is not modeled. The presence of the blade is taken into account by means of momentum sources, which are introduced into the laminar Navier-Stokes equations. In other words, in the ACM approach aerodynamic loads do not result from the solution of fluid motion equations. These loads can come, for example, from the blade element theory. The technique devised by Rogowski [10] is still being developed. In this article, the authors want to show that the proposed method can correctly determine the velocity field around the rotor and behind the rotor based on the set aerodynamic force function (aerodynamic load as a function of the azimuth). The function of aerodynamic forces used in the presented research was created based on the experimental measurements of Strickland *et al.* [6]. For a given rotor position determined using an azimuth θ, the aerodynamic force components are interpolated and entered into the NS equations as:

$$S_{x,y} = \frac{F_{x,y}}{V_c} \tag{3}$$

where: V_c is the volume of the mesh cell, F_x and F_y are aerodynamic force components in the CFD solver system. The ACM model has been implemented in the commercial solver, ANSYS Fluent, which uses the Cartesian coordinate system. The geometrical model of the rotor tested in this work is related to the Cartesian coordinate system as shown in Figures 2–4. In the Cartesian coordinate system, the components of aerodynamic forces are expressed as:

$$F_x = F_N \sin\theta - F_T \cos\theta \tag{4}$$

$$F_y = -F_N \cos\theta - F_T \sin\theta \tag{5}$$

The aerodynamic forces defined by means of Equations (4)–(5), presented in the result section 4, have been normalized:

$$CF_{x,y} = \frac{F_{x,y}}{0.5\rho c} V_0^2 \tag{6}$$

where: ρ is the fluid density.

3.3. Mesh distribution

Both the ACM approach and full CFD models require the use of calculation grids. The grid used for the URANS approach with the k-ε RNG turbulence model and for the laminar model is shown in Figures 5a and 5b. This grid consists of a structural mesh near the edge of the rotor blade and a non-structural mesh in the remaining area. The use of the structural grid provides a better representation of the boundary layer near the edge of the blade. During all simulations, the wall $y+$ parameter was kept less than 1. Figure 5c presents the grid used for a 3D simulation with the SAS model. The grid distribution in the plane perpendicular

to the rotor axis of rotation is the same as in the case of 2D CFD simulations (the same as presented in Figures 5a and 5b). The thickness of the three-dimensional computational domain has a length equal to two chords of the blade. Figures 5d to 5f present the mesh distribution for the ACM approach. Figure 5f shows the densest resolution of the grid near the cell into which the momentum sources are introduced. The number of items for the 3D mesh is 3.9 million, for the 2D mesh it is 131 958 items, whereas in the case of the ACM model, the number of items is 43 707. All the grids presented in this article were thoroughly investigated due to the cell density. A detailed description of these tests and a detailed description of these grids can be found in the articles [7, 10].

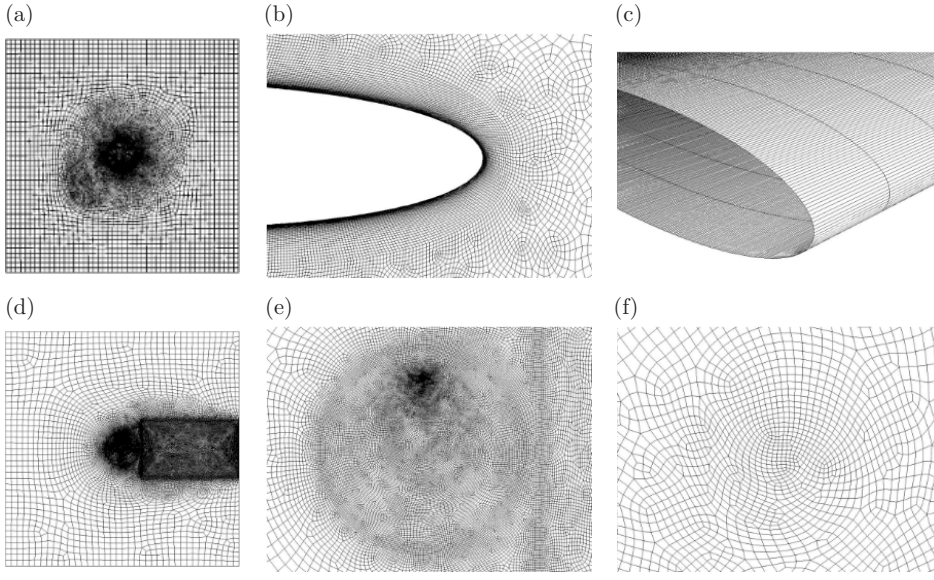

Figure 5. Mesh for full CFD models (Figures a–c) and mesh for ACM model (Figures d–f)

4. Results

4.1. Aerodynamic blade loads

This chapter presents a comparison of the aerodynamic blade loads obtained by means of: the laminar model, the SAS approach and the k-ε RNG turbulence model. The results obtained are compared with the experimental results of Strickland at al. [6]. As mentioned in Chapter 3.2, in the case of the ACM model, the aerodynamic blade loads were not determined. The components of aerodynamic blade loads, in the Cartesian coordinate system, were presented in a dimensionless form (according to Equation (6)) in Figure 6. The azimuth changes from 0 to 360°. However, Figure 6 shows the results for the azimuth in the range from 0 to 450°. It was done to show that the blade loads change the same in each rotation of the rotor (they are repeated in every rotation). As can

be seen in Figure 6, the results of the CF_x force component obtained by means of different numerical approaches are convergent with the experimental values. Some discrepancies are visible in the case of the CF_y component in the azimuth range between 100 and 360°. In the azimuth range up to 300°, it seems that the best results of the CF_y force component are given by the SAS approach. The results of aerodynamic blade loads presented in Figure 6 obtained with the laminar model are amazingly good. We can see that there are considerable oscillations of aerodynamic blade loads resulting from the vortex structures that are formed on the blade surfaces, averaged by *e.g.* the RNG k-ε model. However, these aerodynamic loads oscillate around the experimental values or around values calculated by other methods used.

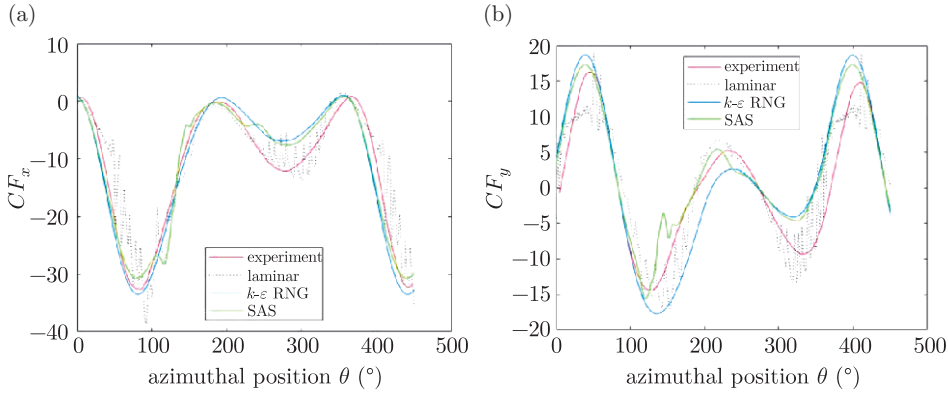

Figure 6. Aerodynamic blade load components. Comparison between full CFD approach and experimental data [1]

4.2. Velocity profiles

Figure 7 presents the profiles of the flow velocity component V_x obtained at a distance of one rotor diameter after the rotor. The velocity components were normalized by the undisturbed flow velocity V_0. The comparison of numerical and experimental results confirms the effectiveness of the methods used for analyzing the aerodynamic wake downstream behind the rotor. The ACM model also gives very good quantitative velocity results.

4.3. Static pressure distribution

As can be seen in Figure 6, the blade load component values in the azimuth range between 180 and 360 are rather smaller compared to the values of these forces in the remaining rotor area. In the trade literature, the rotor area in the azimuth range between 0 and 180° is commonly referred as the upwind part of the rotor while the remaining part is called the downwind part of the rotor. In the upwind part of the rotor, the flow is less disturbed than in the downwind part.

Figures 8–9 present the static pressure distributions for the upwind and downwind parts of the rotor, respectively. The pressure differences between these

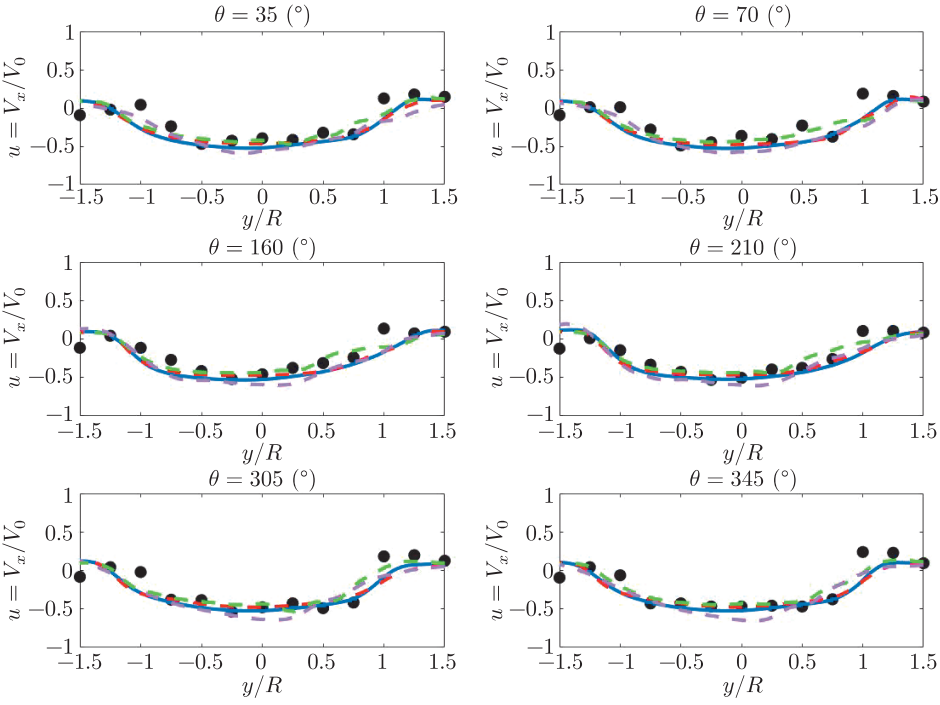

Figure 7. Velocity profiles downstream behind the rotor: experiment (black circles), ACM (blue solid lines), *k*-ε RNG (red dashed lines), laminar (magenta dashed lines), SAS (green dashed lines)

areas are expressive. Figures 8f9 also show the pressure distributions obtained by various numerical methods. If we compare the pressure distributions for the azimuth of 80°, they look very similar. This is related to the components of the aerodynamic blade loads CF_x and CF_y, which in the range of about 60–100° are almost the same for all calculation methods and for the experiment (*cf.* Figure 6). The ACM model indicates pressure results similar to the laminar model and SAS. Employing the *k*-ε RNG turbulence model the pressure is more smooth in the whole azimuth range. The results obtained by means of the laminar model and the SAS model indicate the appearance of flow instabilities near the trailing edge of the azimuth of 120°. This is not visible in the case of the two-equation *k*-ε RNG model. Many works indicate the possibility of flow detachment in this part of the rotor area, *e.g.* [15]. Depending on the rotor, the operating conditions (tip speed ratio) of this phenomenon may be more or less strong. This is a surprising effect because, according to previous observations [4], for the optimal tip speed ratios, the local blade angles of attack should be small and the stall phenomenon should not occur.

4.4. Vorticity magnitude

Another method of assessing the velocity field used in this work is to compare the vorticity magnitude distributions (Figure 10). The vorticity describes the

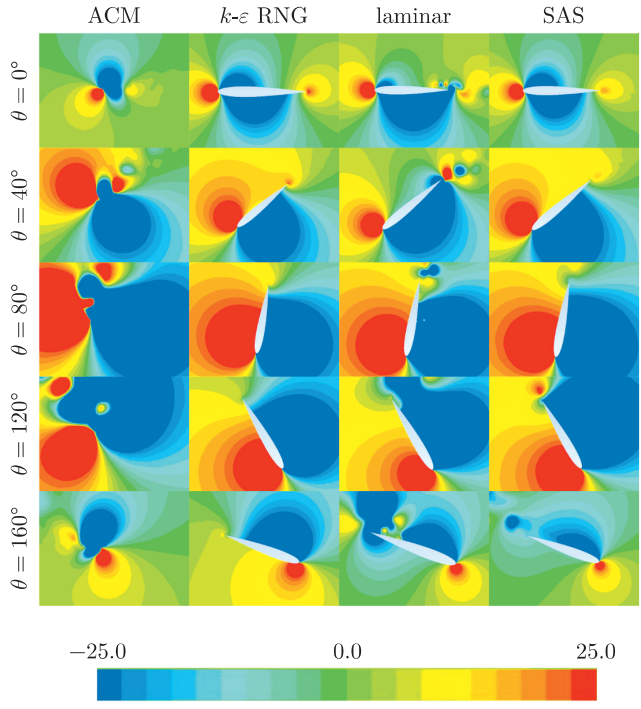

Figure 8. Static pressure distributions for rotor upwind part

tendency of the flow field to rotate. In fluid mechanics the vorticity pseudovector describes the local spinning motion of the flow near some point. Mathematically, in the Cartesian coordinate system, this vector can be defined as:

$$\vec{\omega} = \nabla \times \vec{v} = \left(\frac{\partial v_z}{\partial y} - \frac{\partial v_y}{\partial z} \frac{\partial v_x}{\partial z} - \frac{\partial v_z}{\partial x} \frac{\partial v_y}{\partial x} - \frac{\partial v_x}{\partial y} \right) \tag{7}$$

where: ∇ is the del operator, $\vec{v}$ is the velocity field. In the case of a two-dimensional flow this vector has only a z component:

$$\vec{\omega} = \nabla \times \vec{v} = \left(\frac{\partial v_y}{\partial x} - \frac{\partial v_x}{\partial y} \right) \overrightarrow{e_z} \tag{8}$$

Figure 10 shows contour maps of the vorticity magnitude, *i.e.* the square root of the vorticity vector described by Equation (8). The history of the vorticity magnitude shown in this figure indicates that the velocity field in the upwind part of the rotor is slightly disturbed. In the second part of the rotor, the interaction between the aerodynamic wake created by the rotor blade in the upwind part and the same blade is visible (wake-blade interaction). Comparing the aerodynamic wakes provided by the SAS and ACM models we can observe an amazing compatibility. It seems that it is much more reliable than in the case of the k-ε RNG model. The aerodynamic wake provided by the laminar model is, as expected, heavily disturbed. This model is not equipped with the "mathematical

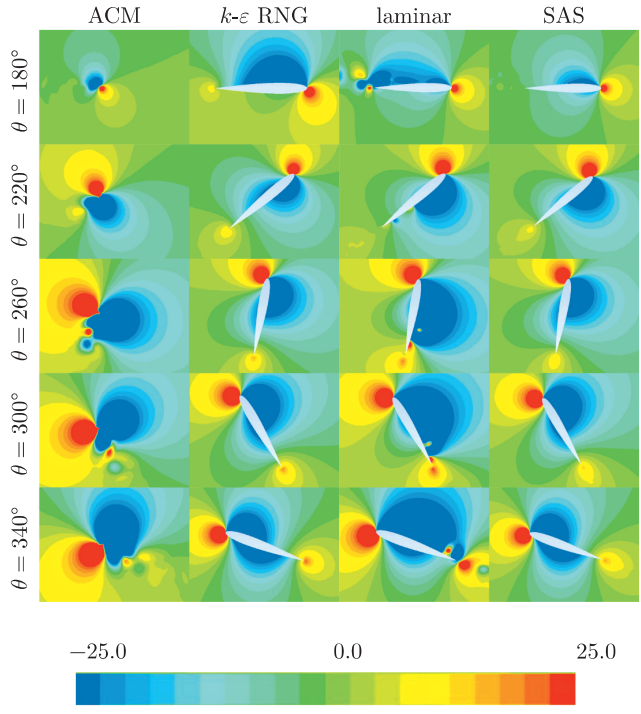

Figure 9. Static pressure distributions for rotor downwind part

mechanism" of dissipative turbulent kinetic energy as in the case of the RNG model.

To better understand the phenomenon of blade-wake interaction, the advantages of the SAS model, which in the case of an unstable flow behaves like a large eddy simulation (LES) model, and the three-dimensional flow model were used. Figure 11 shows the history of vorticity in the area of the three-dimensional Darrieus-type rotor. The figure shows vortex iso-surfaces with the same value (0.151/s) but opposite turns. The blue color suggests the clockwise vorticity direction and the red color the opposite direction.

A flow instability appears for the azimuth of 120–140°. This resulting flow instability evolves and moves with the main stream. Since the velocity of the rotor blade is larger than the main stream velocity, the blade-wake interaction is visible for the azimuth of around 180–200°. The second but smaller blade-wake interaction is visible near the azimuth of 0°.

5. Conclusions

The purpose of this work was to estimate the velocity field around a one-bladed vertical-axis wind turbine using full CFD models and the author's ACM method. The results presented in this article have shown that:

- The advantage of testing a single-bladed rotor is the ability to analyze the interaction of the aerodynamic wake with a rotor blade. The analyses carried

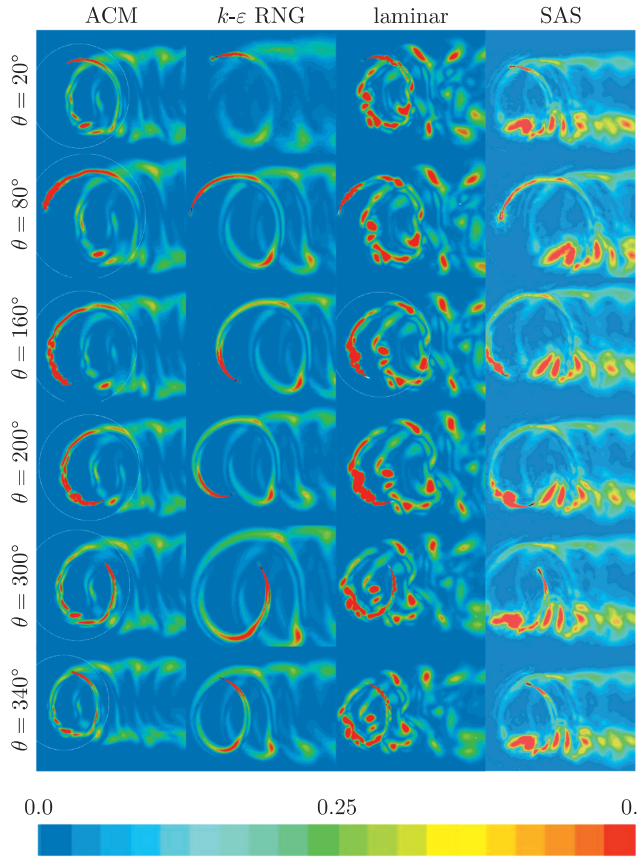

Figure 10. Contour maps of vorticity magnitude for different numerical approaches

out by the authors of this article have shown that the aerodynamic wake behind a vertical-axis wind turbine is very complicated compared to rotors of classic wind turbines with a horizontal axis of rotation.

- Rotors of the Darrieus-type, due to large fluctuations in aerodynamic forces, cannot be tested using the RANS approach.
- The use of standard turbulence models, such as *e.g.* the k-ε family, is not sufficient to study the aerodynamic phenomena of the Darrieus rotor. The SAS model shows many more details of the flow.
- The ACM model gives satisfactory results in the flow field. They are comparable with other CFD methods. The ACM model is further studied in order to be able to estimate the aerodynamic forces on the basis of given profile characteristics. The intention of the authors of the paper is also to study three-dimensional rotors using the developed method.
- In its present form, the ACM method is suitable for testing mixers of some types.
- The laminar model surprisingly well predicts the aerodynamic blade loads and the velocity profiles downstream behind the rotor. Rogowski [16] has also proved

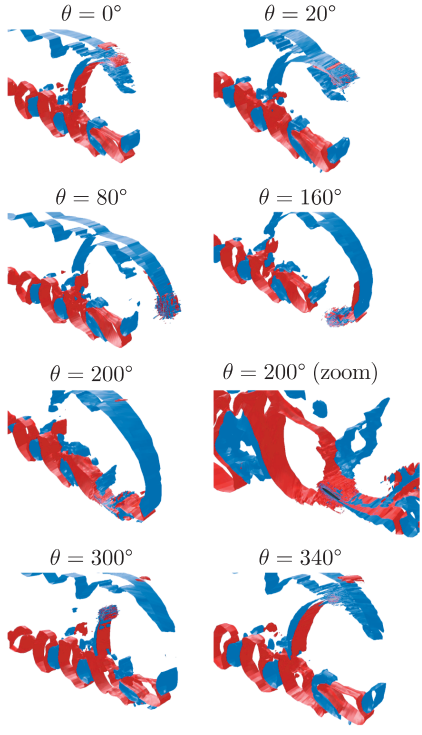

Figure 11. Iso-surfaces of vorticity for SAS simulations

this in the case of another single-bladed rotor. This provides the basis for testing the transitional laminar-turbulent model.

Acknowledgements

The presented numerical computations were performed in the Interdisciplinary Centre for Mathematical and Computational Modeling of the Warsaw University. The current work was prepared as part of the computing grant GB73–5.

References

[1] Szuster J T 2000 *Wind generators with vertical axis of rotation*, National Forum of Renewable Energy, Łódź (in Polish)
[2] Darrieus G J M 1931 *U. S. Patent 1834018*
[3] Madsen H A, Paulsen U S and Vitae L 2012 *J. Phys.: Conf. Ser.* **555** 12065
[4] Paraschivoiu I 2002 *Wind Turbine Design With Emphasis on Darrieus Concept*, International Press, Canada
[5] Castelin D 2015 *Dynamic stall on vertical Axis Wind Turbines*, MSc Thesis, TU Delft
[6] Strickland J H, Smith T and Sun K 1981 *A Vortex Model of the Darrieus Turbine: An Analytical and Experimental Study*, Technical Report SAND'81–7017
[7] Rogowski K, Hansen M O L, Maroński R and Lichota P 2016 *J. Phys.: Conf. Ser. 753* 22050
[8] Rogowski K, Maroński R and Hansen M O L 2018 *J. Theor. App. Mech.* **51** (1) 203
[9] Rogowski K, Hansen M O L, Hansen R, Piechna J and Lichota P 2018 *J. Phys.: Conf. Ser.* **1037** 22019

[10] Rogowski K 2018 *J. Phys.: Conf. Ser.* **1101** 12028
[11] Strickland J H, Webster B T and Nguyen T 1979 *A Vortex Model of the Darrieus Turbine: An Analytical and Experimental Study*, Technical Report SAND'79–7058
[12] Strickland J H, Webster B T and Nguyen 1979 *J. Fluid Eng.* **101** 500
[13] Rogowski K 2014 *Analysis of Performance of the Darrieus Wind Turbines*, Ph.D. Thesis, Warsaw
[14] Rogowski K and Maroński R 2015 *J. Theor. App. Mech.* **53** (1) 37
[15] Bangga G, Hutomo G, Wiranegara R and Sasongko H 2017 *J. Mech. Sc. and Techn.* **31** (1) 261
[16] Rogowski K 2018 *J. Mech. Sc. and Techn.* **32** (5) 2079